



ARL-TR-8140 • SEP 2017



The Use of Ferroelectric Ceramics to Charge Small Capacitor Banks

by Peter Bartkowski and Paul Berning

Approved for public release; distribution is unlimited.

NOTICES

Disclaimers

The findings in this report are not to be construed as an official Department of the Army position unless so designated by other authorized documents.

Citation of manufacturer's or trade names does not constitute an official endorsement or approval of the use thereof.

Destroy this report when it is no longer needed. Do not return it to the originator.



The Use of Ferroelectric Ceramics to Charge Small Capacitor Banks

by Peter Bartkowski and Paul Berning
Weapons and Materials Research Directorate, ARL

REPORT DOCUMENTATION PAGE

Form Approved
OMB No. 0704-0188

Public reporting burden for this collection of information is estimated to average 1 hour per response, including the time for reviewing instructions, searching existing data sources, gathering and maintaining the data needed, and completing and reviewing the collection information. Send comments regarding this burden estimate or any other aspect of this collection of information, including suggestions for reducing the burden, to Department of Defense, Washington Headquarters Services, Directorate for Information Operations and Reports (0704-0188), 1215 Jefferson Davis Highway, Suite 1204, Arlington, VA 22202-4302. Respondents should be aware that notwithstanding any other provision of law, no person shall be subject to any penalty for failing to comply with a collection of information if it does not display a currently valid OMB control number.

PLEASE DO NOT RETURN YOUR FORM TO THE ABOVE ADDRESS.

1. REPORT DATE (DD-MM-YYYY) September 2017		2. REPORT TYPE Technical Report		3. DATES COVERED (From - To) 1 October 2016–30 September 2017	
4. TITLE AND SUBTITLE The Use of Ferroelectric Ceramics to Charge Small Capacitor Banks				5a. CONTRACT NUMBER	
				5b. GRANT NUMBER	
				5c. PROGRAM ELEMENT NUMBER	
6. AUTHOR(S) Peter Bartkowski and Paul Berning				5d. PROJECT NUMBER AH80	
				5e. TASK NUMBER	
				5f. WORK UNIT NUMBER	
7. PERFORMING ORGANIZATION NAME(S) AND ADDRESS(ES) US Army Research Laboratory ATTN: RDRL-WMP-E Aberdeen Proving Ground MD 21005-5066				8. PERFORMING ORGANIZATION REPORT NUMBER ARL-TR-8140	
9. SPONSORING/MONITORING AGENCY NAME(S) AND ADDRESS(ES)				10. SPONSOR/MONITOR'S ACRONYM(S)	
				11. SPONSOR/MONITOR'S REPORT NUMBER(S)	
12. DISTRIBUTION/AVAILABILITY STATEMENT Approved for public release; distribution is unlimited.					
13. SUPPLEMENTARY NOTES					
14. ABSTRACT Shock-induced depolarization of ferroelectric generators (FEGs) was used to charge a small capacitor bank. Lateral and longitudinal orientations of the FEG were investigated. The shock was provided by a sheet of explosives sandwiched with steel plates. Two different mounting concepts were explored. The first mounted the FEG to the edge of the sandwich using a machined coupler, and the second mounted the FEG to the face of the sandwich. The peak charge transferred from the PZT 95/5 material was measured to be 26.8 $\mu\text{C}/\text{cm}^2$.					
15. SUBJECT TERMS shock depolarization, ferroelectric generator, ferroelectric ceramic, explosive, charge transfer					
16. SECURITY CLASSIFICATION OF:			17. LIMITATION OF ABSTRACT UU	18. NUMBER OF PAGES 32	19a. NAME OF RESPONSIBLE PERSON Peter Bartkowski
a. REPORT Unclassified	b. ABSTRACT Unclassified	c. THIS PAGE Unclassified			19b. TELEPHONE NUMBER (Include area code) 410-278-0210

Contents

List of Figures	iv
List of Tables	iv
1. Introduction	1
2. Background	1
3. Material	2
4. Experimental Setup	3
5. Experimental Data	5
6. Conclusions	12
7. References	14
Appendix. Experimental Setups	16
List of Symbols, Abbreviations, and Acronyms	24
Distribution List	25

List of Figures

Fig. 1	PZT 95/5 ferroelectric ceramic bar	2
Fig. 2	FEG surface mount soldered to circuit board	3
Fig. 3	Load circuit board with capacitors.....	4
Fig. 4	FEG charging circuit.....	4
Fig. 5	Explosive sandwich dimensions (inches)	5
Fig. 6	Edge shock experiment orientation with lateral FEG placement.....	6
Fig. 7	Face shock experiment orientation with longitudinal FEG placement	6
Fig. 8	Capacitor voltages recorded during edge experiments	8
Fig. 9	Capacitor voltage rise recorded during edge experiments	9
Fig. 10	Capacitor voltages recorded during face experiments	10
Fig. 11	Experiment FEG8 orientation	10
Fig. 12	Tandem FEG experiment FEG9 orientation	11
Fig. 13	Tandem FEG voltage recorded during experiment FEG9	11
Fig. A-1	Experiment FEG1	17
Fig. A-2	Experiment FEG2	18
Fig. A-3	Experiment FEG3	19
Fig. A-4	Experiment FEG4	19
Fig. A-5	Experiment FEG5	20
Fig. A-6	Experiment FEG6	20
Fig. A-7	Experiment FEG7	21
Fig. A-8	Experiment FEG8	22
Fig. A-9	Experiment FEG9	23

List of Tables

Table 1	Experimental summary	7
---------	----------------------------	---

1. Introduction

Ferroelectric generators (FEGs) provide a very stable form of electrical energy storage with very long lifespan (decades) and zero maintenance requirements. These factors make FEGs very desirable as an energy storage device. While the FEGs have a very long life, they have relatively low energy density compared to many battery technologies. For this effort, we investigated the use of FEGs to charge a small capacitor bank.

2. Background

A ferroelectric (FE) material is a type of dielectric that exhibits a remanent polarization when poled by an electric field. The effect is analogous to a ferromagnetic (FM) material, which retains a remanent polarization when poled by a magnetic field. Both types of permanent polarization represent stored energy that can, at least to some extent, be released by compressive shock loading. A device that utilizes an FE material for this purpose is referred to as an FEG and a device that utilizes an FM material for this purpose is referred to as a ferromagnetic generator (FMG). The idea of using an FE material as an energy source was first proposed in the 1950s.¹

The analogy between an FE material and an FM material is not perfect. While in theory an FE material can retain an electric field just as an FM material retains a magnetic field, in practice ambient charges collect on the electrodes of an FE material to the point where the electric field is cancelled. It is the bound surface charges that represent the stored energy in an FEG material, rather than the electric field. Driving some or all of the FE material into a non-FE state through compressive shock loading will release some or all of the bound charges in an irreversible fashion.

Most commercially available FE materials, such as $\text{Pb}(\text{Zr}_{0.52}\text{Ti}_{0.48})\text{O}_3$ (PZT), are designed for use in piezoelectric devices, where elastic loading is used to free bound charges, reversibly, or alternately a voltage is applied to change the strain state. These types of materials are optimized for this effect and do not as a rule completely depolarize when used as an FEG² and are thus energy inefficient. In response to this, decades ago Sandia National Laboratories developed an alternate material, $\text{Pb}(\text{Zr}_{0.95}\text{Ti}_{0.05})\text{O}_3$ (doped with 2% Nb), referred to as “PZT 95/5”, that transitions from an FE phase to an anti-ferroelectric phase (AFE) phase^{3,4} when shock loaded to a sufficient extent. As an AFE phase exhibits zero net polarization by definition, the material can in theory completely depolarize under shock loading, assuming that a threshold level of shock has been exceeded. The mechanical and electrical

response of this material under shock loading have been extensively studied in the intervening decades.⁵⁻⁷

An FEG in which the shock wave traverses the sample parallel to the polarization axis is referred to as an “axial FEG”.⁸ The devices used in this work are “transverse FEGs”, where the shock wave traverses the sample perpendicular to the polarization vector.^{2,9,10} In a transverse FEG, complete depolarization is achieved once the shock wave (travelling at the nominal acoustic speed of 4.2 km/s)⁵ has swept the entire area of the electrodes. The current output into a short circuit at any given time is proportional to the length of the shock front that intersects the electrodes at that time, so that the pulse shape is entirely geometry-driven.¹⁰

For decades, Sandia National Laboratories was the only source of PZT 95/5 material. Recently, the company TRS Technologies began producing a variant that they claim is superior to Sandia’s version, retaining as much as approximately 33 $\mu\text{C}/\text{cm}^2$ of stored charge versus Sandia’s approximately 28 $\mu\text{C}/\text{cm}^2$.^{2,9} The material in this work comes from TRS Technologies.

The goal of these experiments is to determine the best technique to couple the FEG to the explosive sandwich and measure the amount of charge delivered to a small capacitor bank by the FEG.

3. Material

The PZT 95/5 material was obtained from TRS Technologies in the form of 12.7-mm \times 12.7-mm \times 50-mm bars (Fig. 1). The material was polarized perpendicular to one of the 12.7-mm dimensions. Given the 12.7-mm \times 50-mm dimension of the electrodes and the 33 $\mu\text{C}/\text{cm}^2$ stored charge value, we expected the amount of released charge not to exceed 209.6 μC .

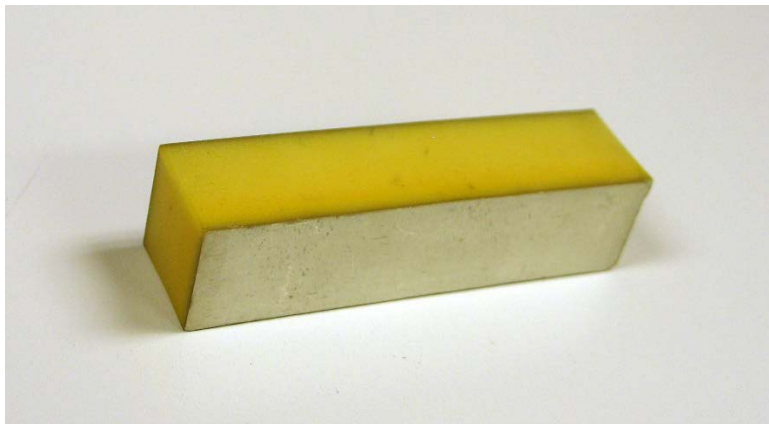


Fig. 1 PZT 95/5 ferroelectric ceramic bar

4. Experimental Setup

The FEG was surface mount soldered onto a custom circuit board (Fig. 2) using a low-temperature solder (Sn42/Bi57.6/Ag0.4) with a 138 °C melting point.¹¹ The solder paste was applied to the electrodes on the FEG and the circuit board and heated in a 165 °C oven. This is well below the curie temperature of approximately 225 °C for the PZT 95/5 material.¹² In one experiment, a silver-filled epoxy was used instead of solder to attach the FEG to the circuit board.



Fig. 2 FEG surface mount soldered to circuit board

Another load circuit board was custom designed to hold 4 47-nF capacitors in parallel yielding a total capacitance of 188 nF (Fig. 3). The maximum released charge of 209.6 μC should have generated a peak capacitor voltage of 1115 V. The 2 boards were electrically connected by 2 16-AWG wires approximately 1.5 m in length. When shocked and depolarized, the released charge from the FEG travels from its circuit board through the connecting wires and charges the load capacitor bank (Fig. 4). For safety, a 1 mega-ohm resistor was placed in parallel with the capacitors to drain energy from them after the experiment was over. The time constant for this exponential decay is 188 ms, several orders of magnitude larger than the 100 μs recording time for the experiment.

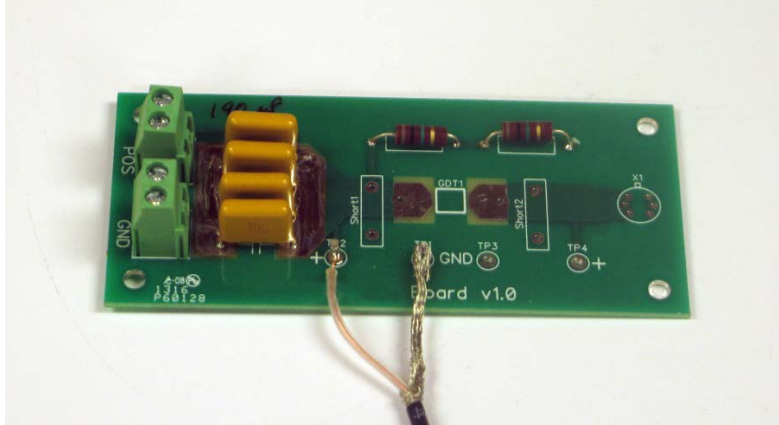


Fig. 3 Load circuit board with capacitors

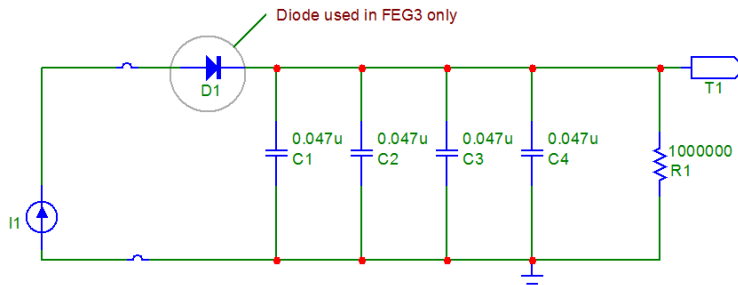


Fig. 4 FEG charging circuit

The depolarizing shock was provided by a sandwich of 3-mm steel plates with 3-mm Primasheet 1000 flexible sheet explosive in the middle (Fig. 5). One steel plate was shorter than the other to expose the Primasheet explosives for initiation. Various orientations of coupling the sandwich to the FEG were investigated using epoxy to adhere parts together with a 0.8-mm-thick G-10 fiberglass insulating layer. The sandwich was command detonated using a RISI RP-80 detonator with an additional 6-mm-diameter piece of 3-mm-thick Primasheet as a booster.

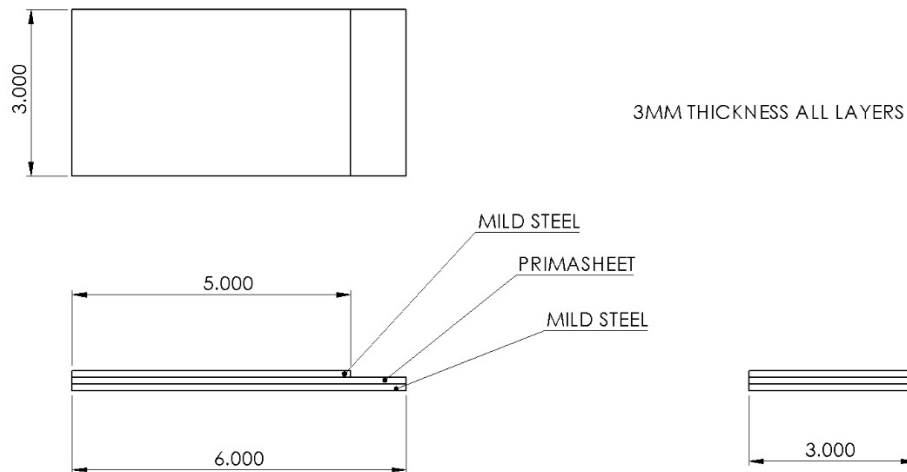


Fig. 5 Explosive sandwich dimensions (inches)

Two data signals were recorded during the experiments. The current traveling through the firing line to the detonator was recorded as well as the voltage of the capacitor bank. Both signals were recorded on a 4GSa/s Agilent Technologies model DS06104A Digital Oscilloscope. For all these experiments, time zero represents the time the current pulse was applied to the detonator.

5. Experimental Data

Two basic methods of shocking the FEG were explored, “edge” and “face”. The edge shock (Fig. 6) utilized a 6061-T6 aluminum or Nylon coupler that was mounted to the edge of the explosive sandwich as an interface between the FEG and the explosive sandwich. Most of the edge shock experiments used a lateral placement of the FEG at the end of the sandwich plates, but one experiment (FEG8) had the FEG in a longitudinal orientation along the side of the sandwich. The face shock technique (Fig. 7) mounted the FEG using epoxy to the face of the steel sandwich plate in either a lateral or longitudinal orientation (see Appendix) to the detonation wave front. All experiments, except the one that used a Nylon coupler, utilized a 0.8-mm-thick G-10 insulator to electrically isolate the sandwich and/or coupler from the FEG. Table 1 is a summary of all experimental data collected.

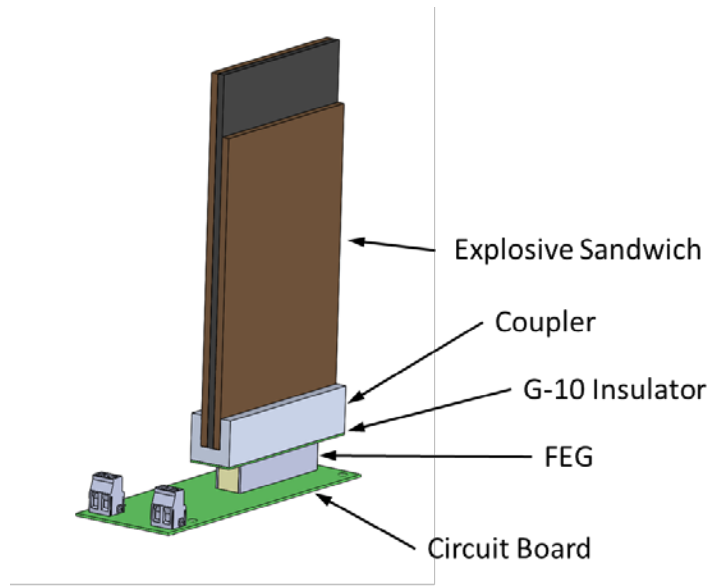


Fig. 6 Edge shock experiment orientation with lateral FEG placement

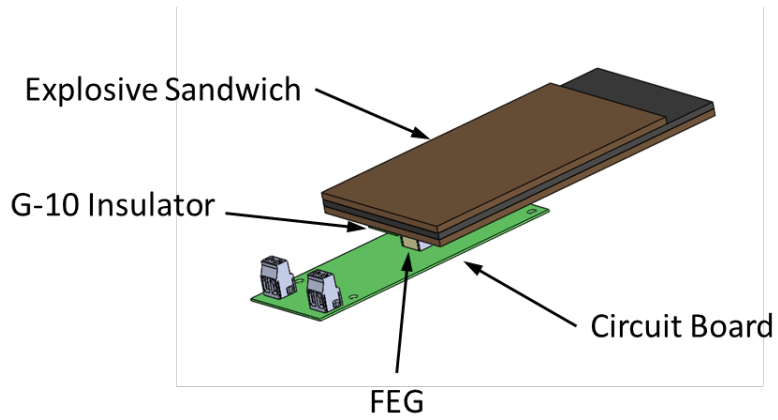


Fig. 7 Face shock experiment orientation with longitudinal FEG placement

Table 1 Experimental summary

Exp no.	Shock (edge/face)	Direction (lat/long)	Risetime (μ s)	Peak V (V)	Charge (μ C)	Notes
1	edge	lateral	3.16	863	162.2	
2	face	longitudinal	3.42	328	61.7	
3	edge	lateral	3.16	906	170.3	Diode to prevent short
4	edge	lateral	3.19	781	146.8	Silver-filled epoxy circuit bond
5	edge	lateral	3.41	894	168.1	Nylon coupler
6	face	longitudinal	5.83	656	123.3	Aluminum buffer bar
7	face	lateral	3.64	818	153.8	
8	edge	longitudinal	8.75	888	166.9	FEG on side of plate
9	edge	long + lat	8.37, 1.17	1250	235.0	2 FEGs, side and end

In all, 5 edge shock experiments were conducted with a lateral orientation of the FEG. Experiments FEG1, FEG3, FEG4, and FEG5 had the FEG on the end edge of the sandwich as shown in Fig. 6. This orientation had the detonation wave arriving nearly simultaneously across the top surface of the FEG. In this case, the FEG will release stored charge as the shock wave travels through the 12.7-mm thickness of the bar. The capacitor voltages recorded during these experiments are shown in Fig. 8. Experiment FEG1 yielded a capacitor voltage of 863 V for 10.5 μ s before the voltage dropped. Inspection of the load circuit board after the experiment indicated that no failures occurred on it during the experiment. Thus we concluded that a short circuit occurred on the FEG circuit board 10.5 μ s after the current peaked. To test this theory, experiment FEG3 was conducted using the same setup as FEG1, except that an 1800 VDC diode was placed in the positive wire between the 2 circuit boards. The diode was oriented to allow the FEG to charge the capacitor bank, but a reverse current would be blocked if a short circuit on the FEG board occurred. The capacitor voltage from experiment FEG3 rose to 906 V and did not rapidly drop as it did in experiment FEG1, confirming the short circuit theory.

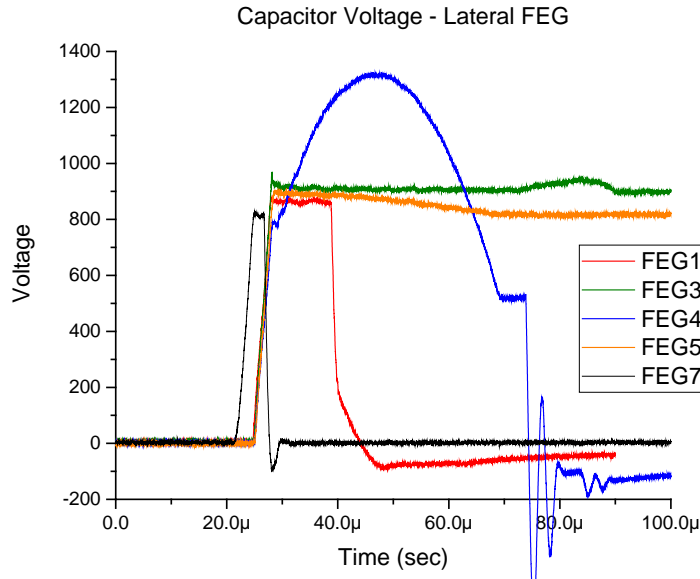


Fig. 8 Capacitor voltages recorded during edge experiments

An alternate method of attaching the FEG to the circuit board was investigated in experiment FEG4. Instead of solder, a conductive silver-filled epoxy was used to electrically and mechanically bond the FEG to the circuit board. While the FEG at first appeared to charge the capacitors as expected to 781 V, the signal rose again in a sinusoidal shape to a peak of 1317 V. At 73.9 μs time, the signal appeared to short circuit. We do not believe the sinusoidal signal was from the FEG, but instead that it was a ground loop created by a connection between the firing line for the detonator and the digital oscilloscope through the 2 connected circuit boards. The rise of the voltage to 781 V was somewhat lower than the other edge shock experiments.

In experiment FEG5, the aluminum coupler was replaced by one made from nylon and the G-10 insulation layer was eliminated. This configuration showed good results with a peak voltage of 894 V and a steady voltage beyond 100 μs , even without the diode as in experiment FEG3.

One face shock experiment with a laterally oriented FEG was conducted. In experiment FEG7, the voltage signal rose in 3.61 μs to a peak voltage of 818 V. This voltage did not last long and appeared to short circuit 1.7 μs after the voltage peaked.

For all of the edge shock experiments, a depolarization speed of 4.2 mm/ μs for the PZT 95/5 should produce a linear signal rise time (0%–100%) of 3.02 μs from a planar shock.⁵ Due to the fact that we are point initiating the Primasheet, we would expect the measured rise times to be somewhat longer due to the curved detonation

front. Figure 9 is an expanded view of Fig. 8, showing the rise of all 5 signals. The rise time of all the edge shock experiments using the aluminum coupler was $3.17 \pm .02 \mu\text{s}$. The one experiment using the nylon coupler (FEG5) had a slightly longer rise time of $3.41 \mu\text{s}$. The face shock experiment of FEG7 had a longer rise time of $3.64 \mu\text{s}$ due to the shockwave traversing the width and depth of the FEG bar.

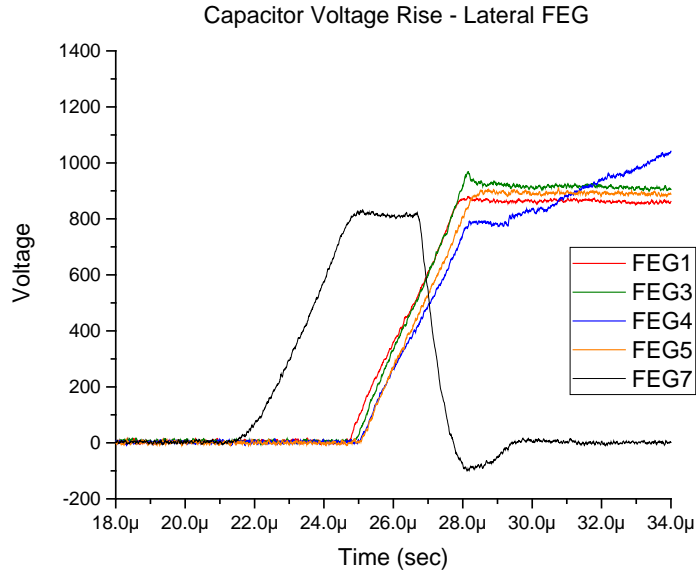


Fig. 9 Capacitor voltage rise recorded during edge experiments

The voltages recorded during the 3 longitudinally oriented FEG shock experiments are shown in Fig. 10. The first 2 longitudinal face shock experiments (FEG2 and FEG6) did not perform well. In this orientation, the explosive shock must travel the 50-mm length of the FEG. The Primasheet 1000 flexible sheet explosive has a detonation velocity of $7.1 \text{ mm}/\mu\text{s}$. We expected the voltage signal from these 2 experiments to have a rise time of $7.04 \mu\text{s}$. Experiment FEG2 appeared to short circuit at $3.85 \mu\text{s}$ after the voltage began to rise. A modification was made to experiment FEG6; a 6.3-mm-thick 6061-T6 aluminum buffer bar was added between the steel plate of the explosive sandwich and the G-10 insulator. This worked somewhat better in that the voltage short circuited a bit later at $5.88 \mu\text{s}$ after the voltage began to rise. However, neither of these experiments appeared to reach peak voltage.

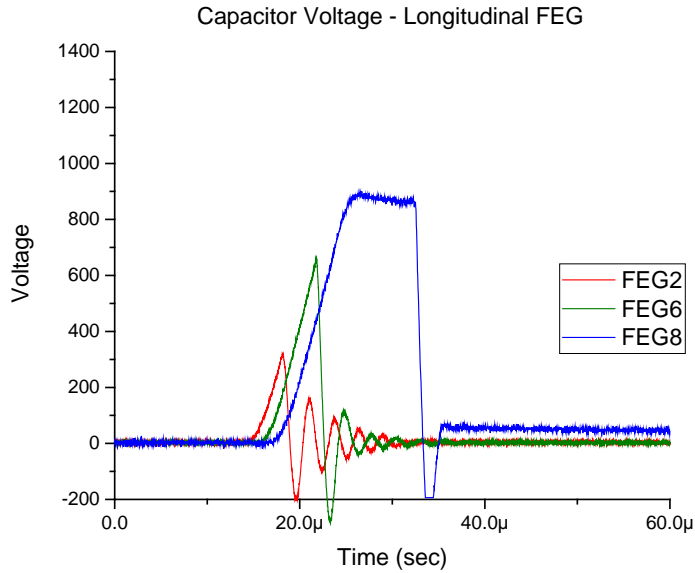


Fig. 10 Capacitor voltages recorded during face experiments

The experiment FEG8 was an edge shock experiment with a longitudinally oriented FEG. The FEG was placed on the side of the sandwich using an aluminum coupler with a G-10 insulator between the coupler and FEG bar (see Fig. 11). As can be seen in Fig. 10, the peak voltage recorded was 888 V and the signal had a rise time of 8.75 μ s. The signal appeared to short circuit 6.55 μ s after the peak was attained.

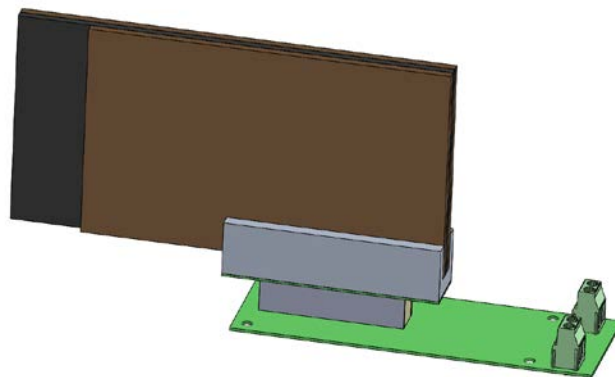


Fig. 11 Experiment FEG8 orientation

With good results from all the edge shock experiments, a final experiment was conducted using 2 FEGs. One was placed in the lateral orientation on the end of the sandwich while a second FEG was placed longitudinally along the side of the sandwich (see Fig. 12). This experiment was a combination of experiments FEG3 and FEG8. Wires were then used to connect the 2 FEG circuit boards to a single

load circuit board. Diodes were used on the positive leads between the boards to prevent any short circuits from discharging the capacitor bank. In this experiment, we expected to see a slow rise time of approximately $7.04 \mu\text{s}$ from the longitudinally oriented FEG, followed by another sharper rise of approximately $3.02 \mu\text{s}$. As can be seen in Fig. 13, the voltage signal does indeed have 2 distinct rises from each of the FEG bars. The first one rises to a voltage of 797 V in $8.37 \mu\text{s}$, with a following rise of 550 V in $1.33 \mu\text{s}$. After a quick pull back, the total sustained voltage is 1250 V .

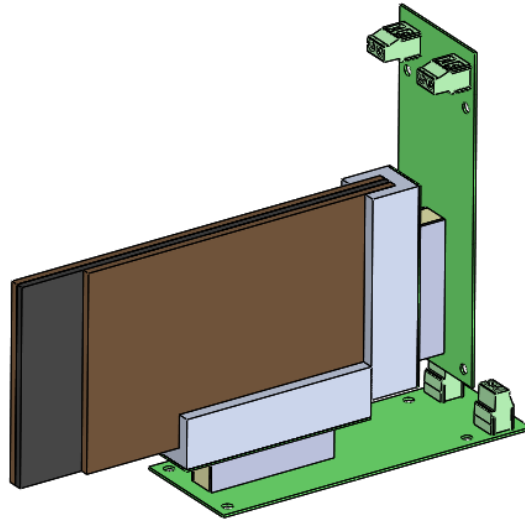


Fig. 12 Tandem FEG experiment FEG9 orientation

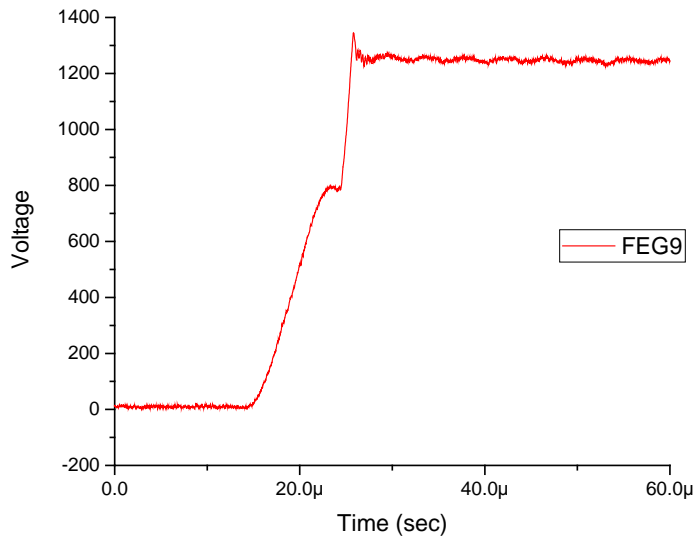


Fig. 13 Tandem FEG voltage recorded during experiment FEG9

6. Conclusions

With the figure of merit being the amount of released charge transferred to the capacitor, in general, the edge shock method with the FEG worked better than the face shock technique. The highest amount of charge transferred was during experiment FEG3, which transferred 170.3 μC of charge. This is 81.2% of our theoretical maximum 209.6 μC . The next best edge shock experiments were FEG5, FEG8, FEG1, and FEG4, which resulted in 80.2%, 79.6%, 77.4%, and 70.0% of charge transferred respectively. The edge shock lateral experiments all produced similar results except for FEG4 that utilized silver-filled epoxy to attach the FEG to the circuit board. At first, one may try attributing the lower transferred charge to the higher resistivity of the silver-filled epoxy compared to the solder used in all the other experiments. However, as a charge source, the FEG should output the same amount of charge to the capacitor regardless of the resistance between the 2 materials.

Both of the longitudinal face shock experiments ended prematurely. Experiments FEG2 and FEG6 did not reach peak current before shorting out. The shock is most likely the cause of the short circuit. Once the shock travels through the FEG material, releasing the stored charge, it then also is transmitted into the circuit board. It is not clear which material is creating the short circuit—the shocked FEG or the fiberglass of the circuit board. The face shock experiment FEG7 had the FEG oriented laterally instead of longitudinally. This experiment did reach peak voltage, but only for 1.7 μs before shorting. It transferred 166.9 μC of charge to the capacitor or 79.6% of the theoretical maximum.

The use of a series diode in the charging circuit helps overcome a short circuit in the FEG or FEG circuit board. When experiment FEG1 was repeated with a diode (FEG3), no short circuiting was observed at the capacitors. Short circuiting may have occurred in the FEG or on the circuit board but the blocking action of the diode prevented the charge stored in the capacitor bank from being affected.

The tandem experiment FEG9 was a combination of the best lateral (FEG3) and longitudinal (FEG8) designs. The combination of the 2 FEGs transferred 235.0 μC of charge to the capacitor bank. With the theoretical value for this experiment being twice that of all the previous experiments, only 56.0% of the available charge was transferred. The longitudinal FEG was first to see the shock and transferred 71.5% of its available charge. The laterally oriented FEG begins to rise but the voltage on the capacitor stops rising 1.17 μs later. This falls short of the expected 3 μs rise time; most likely due to a short circuit developed in the FEG or FEG circuit board. This is a bit unexpected as all the other edge shock experiments

reached peak voltage. Due to this premature short circuit, the laterally oriented FEG only transferred 40.4% of its available charge. But this experiment does prove that multiple FEGs can be placed on a sandwich in different orientations and used to charge a single capacitor bank.

No experiment resulted in more than 81.2% of the theoretical charge from being transferred to the capacitor bank. This correlates to a peak charge transfer of $26.8 \mu\text{C}/\text{cm}^2$. The loss mechanisms affecting the FEG are not currently understood. There are some aspects of the depolarizing process that we may be able to change to improve performance. Some areas for further research include: magnitude of shock, effect of release waves in FEG, and the use of impedance matching materials.

7. References

1. Neilson FW. Bull Am Phys Soc. 1957;2:302.
2. Alberta EF, Michaud B, Hackenburger WS, Freeman B, Hemmert DJ, Stults AH, Altgilbers LL. Development of ferroelectric materials for explosively driven pulsed-power systems. Proceedings of the 17th IEEE Pulsed Power Conference; 2009 Jun 28–Jul 2; Washington, DC. IEEE; c2009 Jan. p. 161–166.
3. Lysne PC. Dielectric properties of shock-wave-compressed PZT 95/5. J App Phys. 1977;48:1020.
4. Lysne PC. Electrical response of a slim-loop ferroelectric ceramic compressed by shock waves. J App Phys. 1978;49:4296.
5. Setchell RE, Chhabildas LC, Furnish MD, Montgomery ST, Holman GT. Dynamic electromechanical characterization of the ferroelectric ceramic PZT 95/5. AIP Conference Proceedings, Shock Compression of Condensed Matter; 1997; Amherst, MA. c1998;429:781.
6. Setchell RE. Recent progress in the shock response of ferroelectric ceramics. AIP Conference Proceedings, Shock Compression of Condensed Matter; 2001; Atlanta, GA. c2002;620:191.
7. Setchell RE, Montgomery ST, Cox DE, Anderson MU. Dielectric properties of PZT 95/5 during shock compression under high electric fields. AIP Conference Proceedings, Shock Compression of Condensed Matter; 2005; Baltimore, MD. c2006;845:278.
8. Furnish MD, Chhabildas LC, Setchell RE, Montgomery ST. Dynamic electromechanical characterization of axially poled PZT 95/5. AIP Conference Proceedings, Shock Compression of Condensed Matter; 1999; Snowbird, UT. c2000;505:975.
9. Setchell RE, Montgomery ST, Chhabildas LC, Furnish MD. The effects of shock stress and field strength on shock-induced depoling of normally poled PZT 95/5. AIP Conference Proceedings, Shock Compression of Condensed Matter; 1999; Snowbird, UT. c2000;505:979.
10. Fu-Ping Z, Jin-Mei D, Yi Z, Yu-Sheng L, Hong-Liang H. Discharge of PZT95/5 ferroelectric ceramics under tilted shock wave compression. AIP Conference Proceedings, Shock Compression of Condensed Matter; 2007; Waikoloa, HI. c2007;955:213.

11. CHIPQUICK SMDLTLFP250T3 datasheet, rev 1.2. [accessed 18 Aug 2017]. <http://www.chipquik.com/datasheets/SMDLTLFP250T3.pdf>.
12. Tuttle BA, Voight A, Scofield TW, Yang P, Zeuch DH, Rodriguez MA. Dielectric properties and depoling characteristics of $\text{Pb}(\text{Zr}_{0.95}\text{Ti}_{0.05})\text{O}_3$ based ceramics: near-critical grain size behavior. Proceedings of the 9th US and Japan Seminar on Dielectric and Piezoelectric Ceramics. 1999;354–358.

Appendix. Experimental Setups

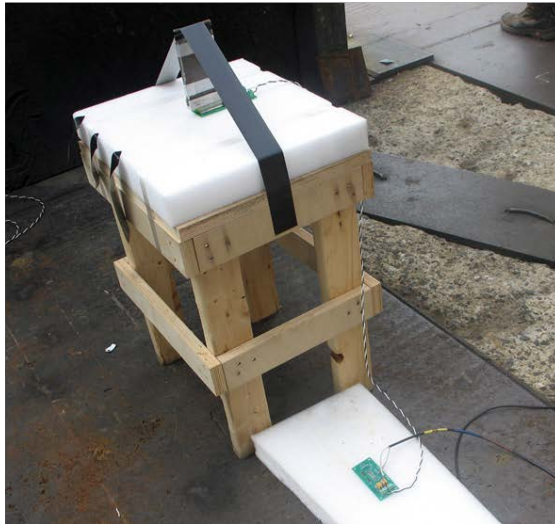
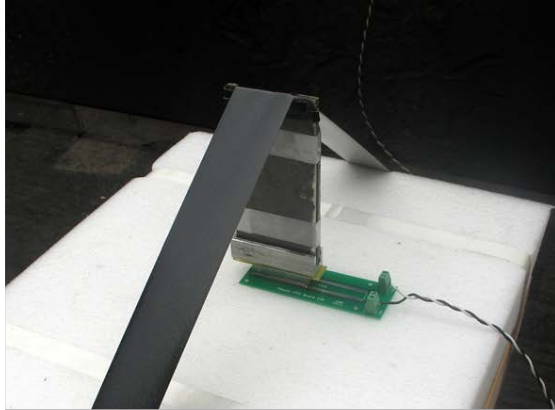
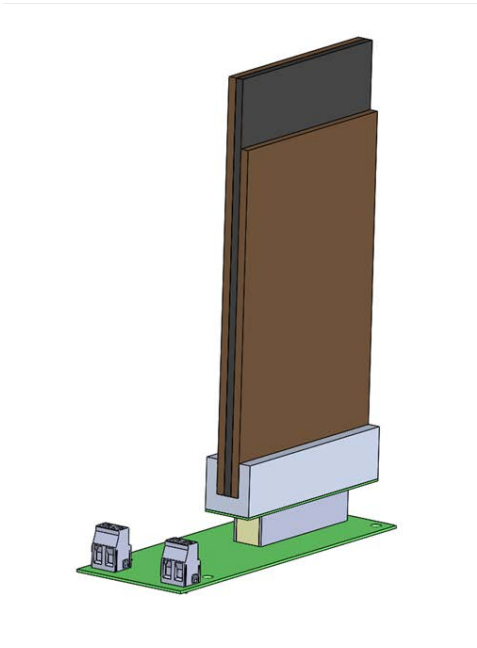


Fig. A-1 Experiment FEG1

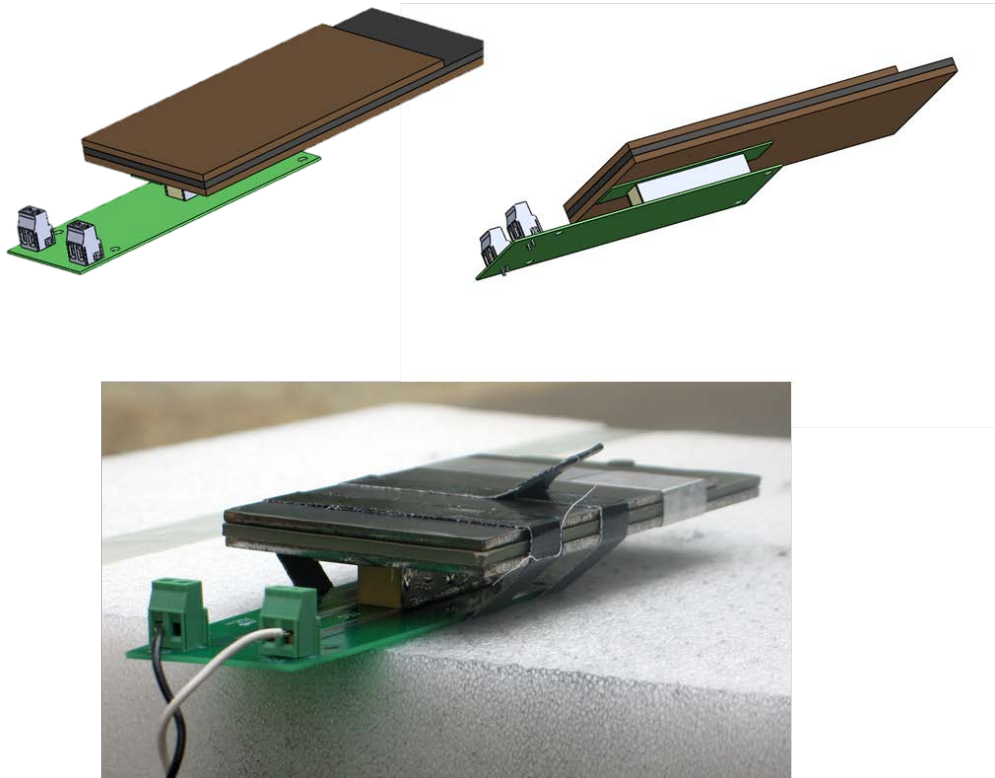


Fig. A-2 Experiment FEG2

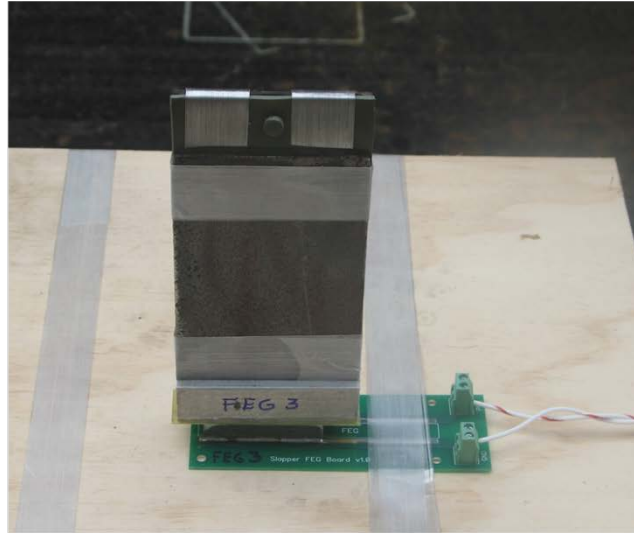
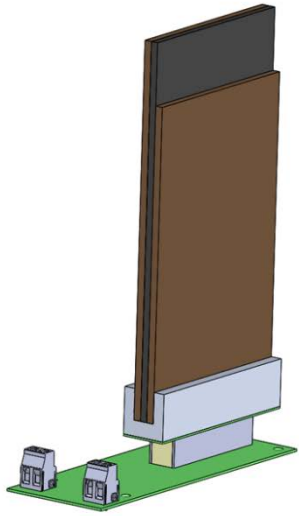


Fig. A-3 Experiment FEG3

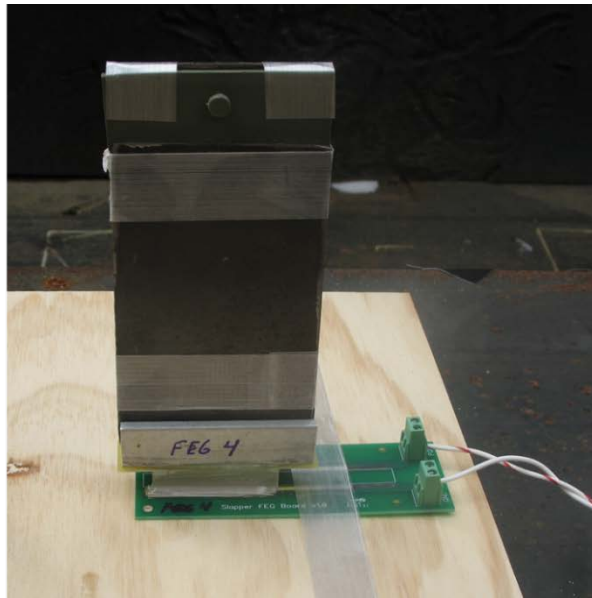
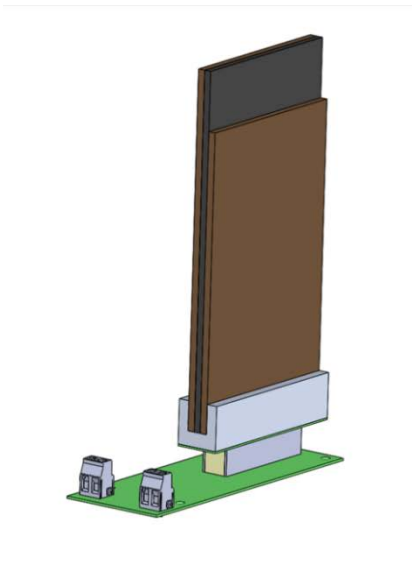


Fig. A-4 Experiment FEG4

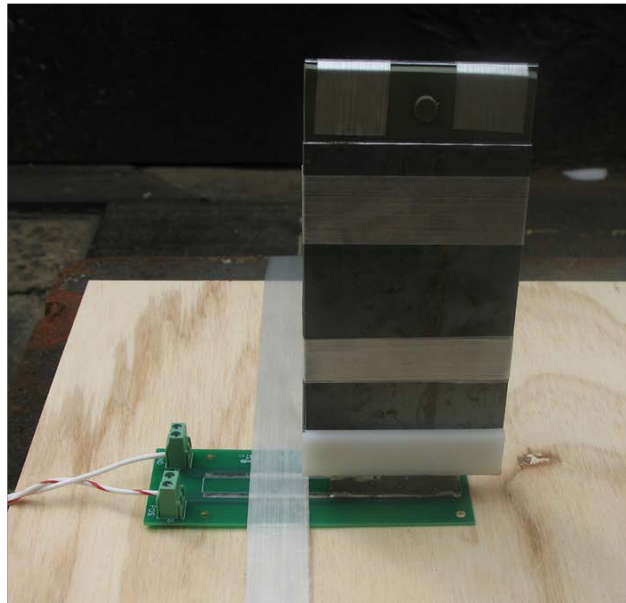
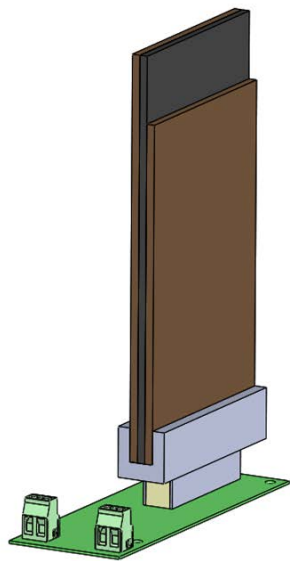


Fig. A-5 Experiment FEG5

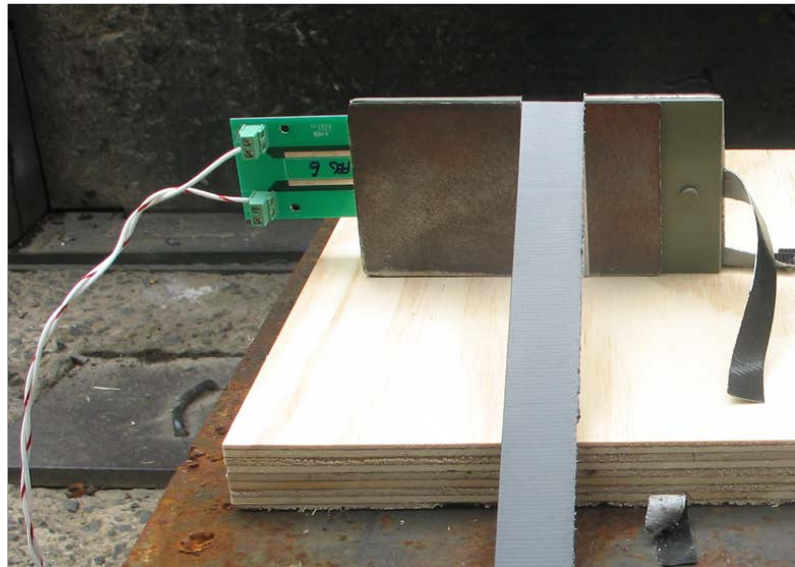
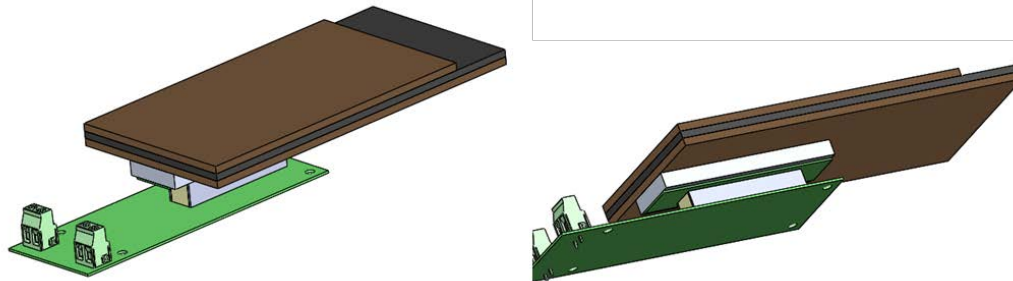


Fig. A-6 Experiment FEG6

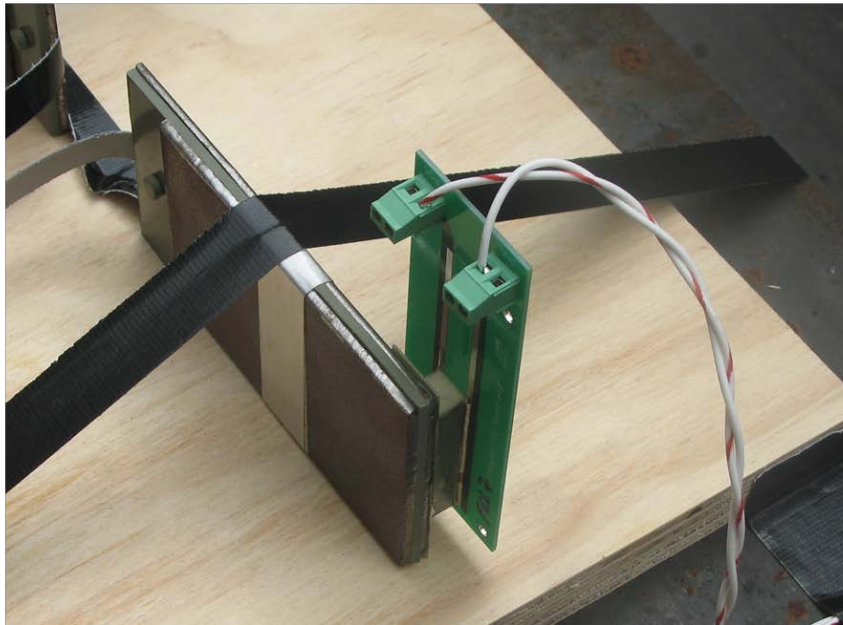
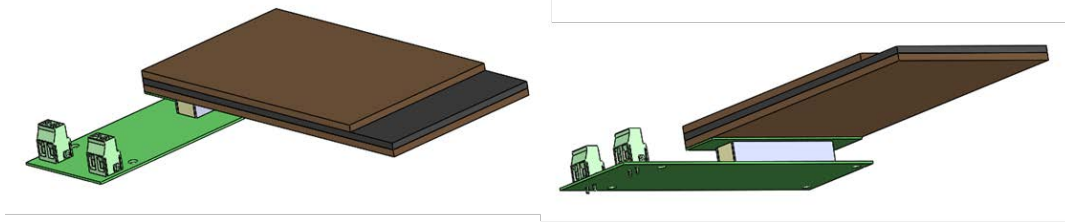


Fig. A-7 Experiment FEG7

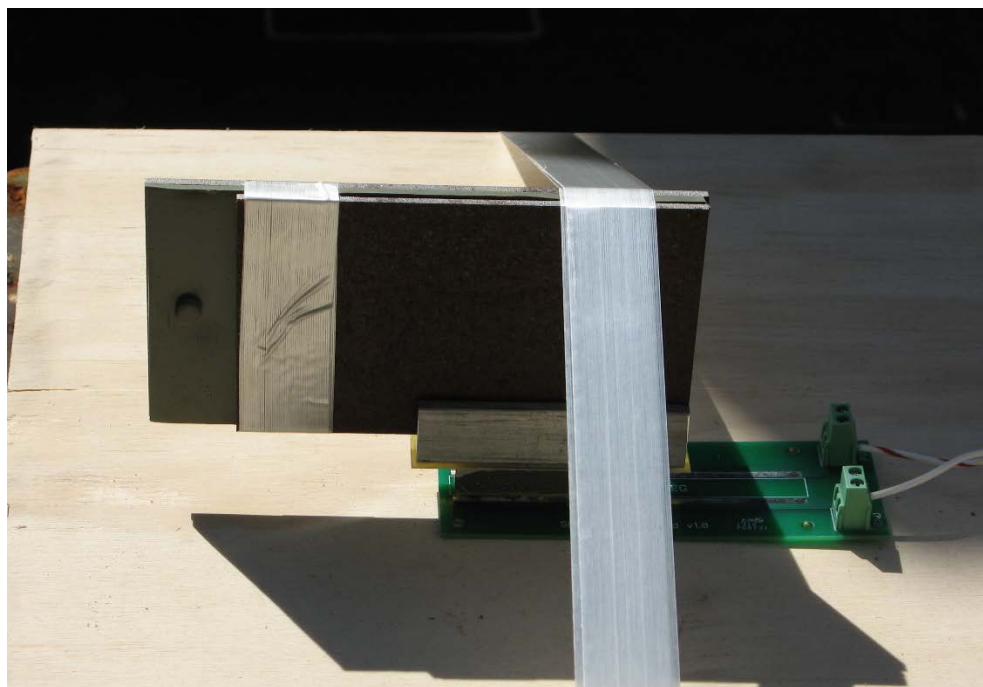
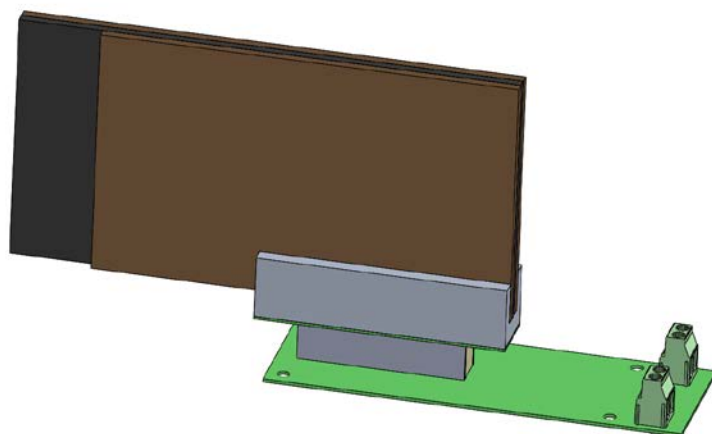


Fig. A-8 Experiment FEG8

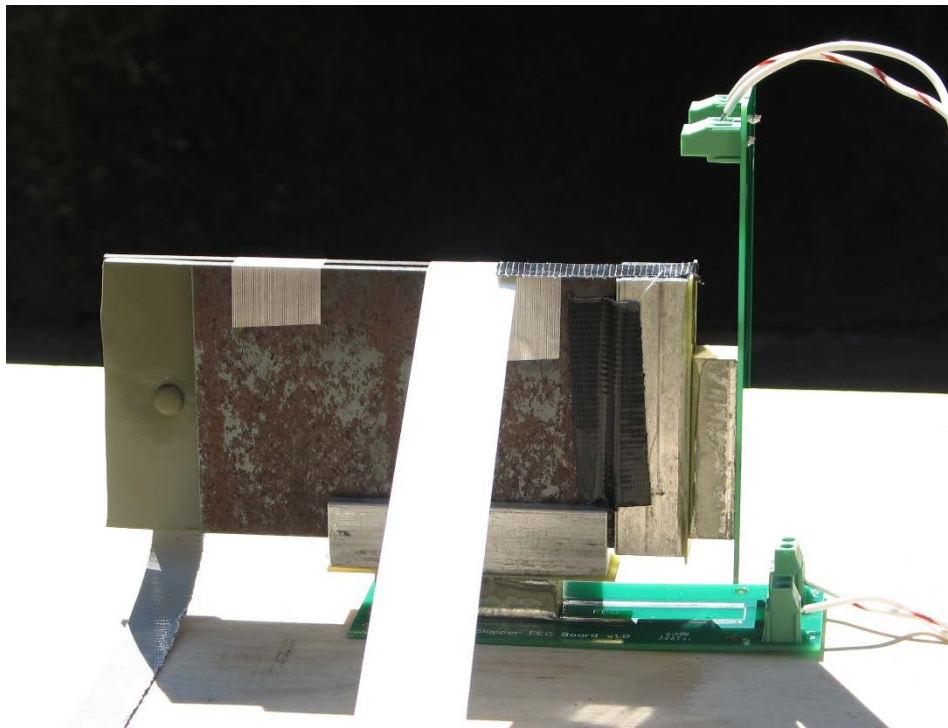
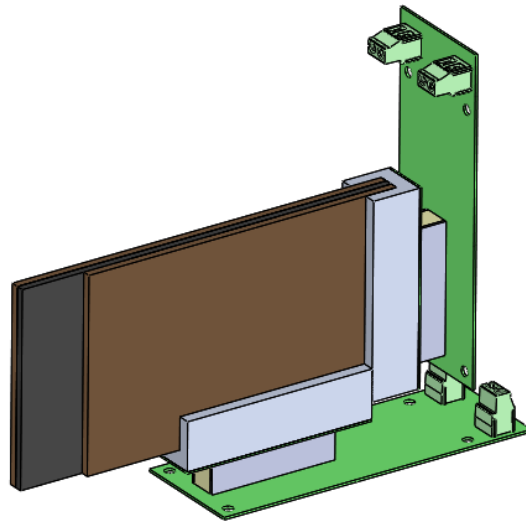


Fig. A-9 Experiment FEG9

List of Symbols, Abbreviations, and Acronyms

AFE	anti-ferroelectric phase
FE	ferroelectric
FEG	ferroelectric generator
FM	ferromagnetic
FMG	ferromagnetic generator

1 DEFENSE TECHNICAL
(PDF) INFORMATION CTR
DTIC OCA

2 DIR ARL
(PDF) RDRL CIO L
IMAL HRA MAIL & RECORDS
MGMT

1 GOVT PRINTG OFC
(PDF) A MALHOTRA

1 DEPT OF THE ARMY
(PDF) NGIC GS MS
C BEITER

1 PEO CS CSS
(PDF) SFAE CSS FP H
D BOCK

1 PROJECT DIRECTOR
(PDF) SFAE GCS M
E BARSHAW

1 PM ABRAMS
(PDF) SFAE GCS HBCT S
J ROWE
R NICOL

2 PM BFVS
(PDF) SFAE GCSS BV
D SPENCER
LTC DEAN

2 PM GCS
(PDF) SFAE GCSS W BCT
M RYZYI
T HOWIE

1 USMC
(PDF) A PURTELL
C/O B SWEDISH

1 DEPT OF THE ARMY
(PDF) TACOM ARDEC
S CHICO

3 DEPT OF THE ARMY
(PDF) TACOM
AMSTA TR R
C FILAR
R RICKERT
A LEE

1 DEPT OF THE ARMY
(PDF) ABERDEEN TEST CENTER
D BLANKENBILLER

106 DIR US ARL
(PDF) RDRL DP
RC BECKER
TW BJERKE
RDRL WMM
JH BEATTY
RDRL WMM A
JJ LA SCALA
DJ O'BRIEN
JP WOLBERT
RDRL WMM B
GA GAZONAS
BM LOVE
RDRL WMM D
BA CHEESEMAN
RE BRENNAN
KC CHO
LR HOLMES
M KORNECKI
SM WALSH
RDRL WMM E
VL BLAIR
SM KILCZEWSKI
JC LASALVIA
PJ PATEL
JJ SWAB
LR VARGAS-GONZALEZ
RDRL WML B
J CIEZAK-JENKINS
F DELUCIA
TA JENKINS
BM RICE
RDRL WML C
KL MCNESBY
TN PIEHLER
B ROOS
GT SUTHERLAND
RDRL WML E
P WEINACHT
RDRL WML H
JC ANGEL
BB AYDELOTTE
TE EHLERS
E KENNEDY
LS MAGNESS
CS MEYER
JF NEWILL
B SCHUSTER
BR SORENSEN
RL SUMMERS

RDRL WMP
DH LYON
JD HOGGE
TT VONG
RDRL WMP A
JW BALL
PR BERNING
SR BILYK
JU CAZAMIAS
MJ COPPINGER
J FLENIKEN
GM THOMSON
WC UHLIG
AR VALENZUELA
LR VANDERHOEF
CM WOLFE
RDRL WMP B
CP HOPPEL
S SATAPATHY
S WOZNIAK
RDRL WMP C
D CASEM
JD CLAYTON
RB LEAVY
SB SEGLETES
AC SOKOLOW
AL TONGE
C WILLIAMS
RDRL WMP D
A BARD
ND BRUCHEY
RL DONEY
ML DUFFY
ST HALSEY
MJ KEELE
DS KLEPONIS
RM MUDD
FJ MURPHY
DW PETTY
CL RANDOW
JW RUNYEON
SJ SCHRAML
BR SCOTT
K STOFFEL
G VUNNI
VS WAGONER
MB ZELLNER

RDRL WMP E
PT BARTKOWSKI
SD BARTUS
MS BURKINS
DB GALLARDY
P GILLICH
DC HACKBARTH
DJ HORNBAKER
J HOUSKAMP
T JONES
C KRAUTHAUSER
MS LOVE
K MCNAB
PM SWOBODA
RDRL WMP F
NM GNIAZDOWSKI
D HOFSTETTER
CJ CUMMINS
DF ERDMAN
RG KARGUS
RDRL WMP G
BE HOMAN
SR KUKUCK
CR PECORA
R SPINK
JB STEWART
RDRL WMM G
JL LENHART
KA MASSER